



National Aeronautics and Space Administration
Goddard Institute for Space Studies
New York, N.Y.



New Methods to Predict Regional Variations of the Mineral and Chemical Composition of Dust Aerosols

Carlos Pérez García-Pando, Jan P. Perlitz, Ron L. Miller

NASA Goddard Institute for Space Studies
Dept of Applied Physics and Applied Math, Columbia University

13th AEROCOM Workshop
Steamboat Springs, Sept-Oct 2014

ACKNOWLEDGEMENTS: Department of Energy and NASA MAP

Motivation

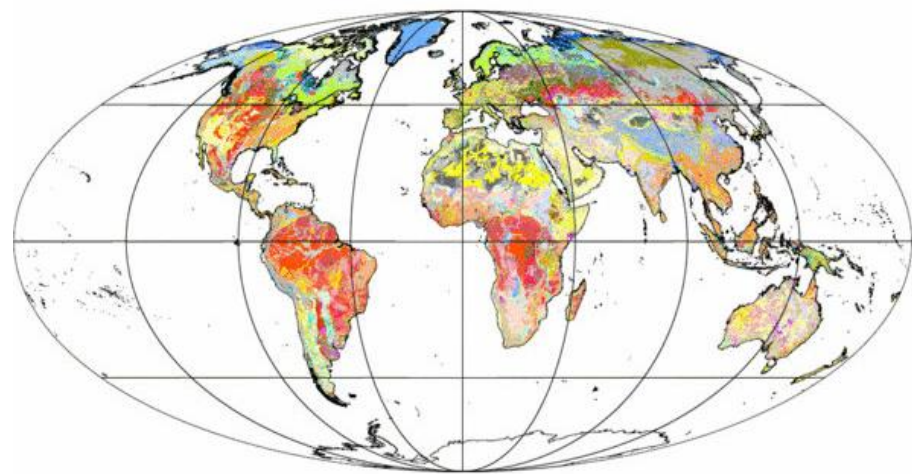
Soil dust aerosols are typically assigned ***globally uniform physical and chemical properties*** within Earth system models, despite known regional variations in the ***mineral content of the parent soil***

Mineral composition of the dust aerosol particles is important to their interaction with climate, including :

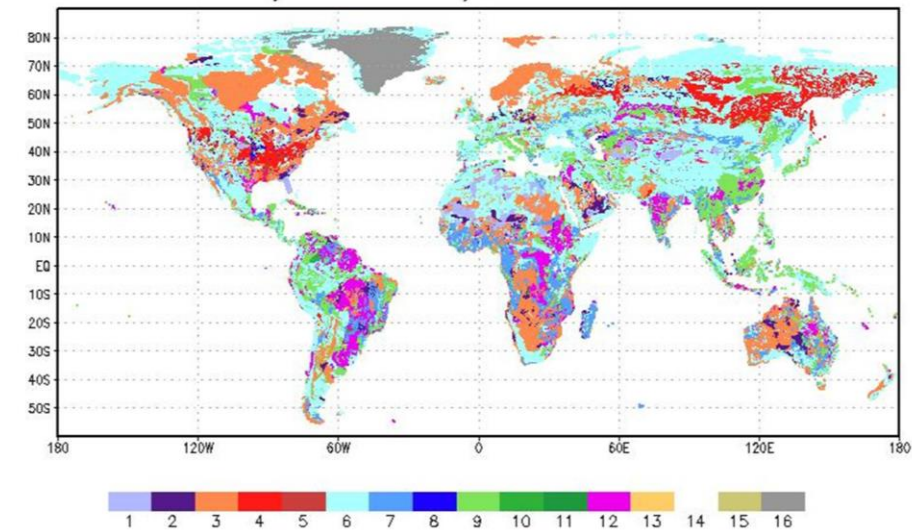
- ***Shortwave absorption*** and ***radiative forcing***
- ***Nucleation*** of cloud droplets and ice crystals
- ***Coating*** by heterogeneous uptake of sulfates and nitrates
- Atmospheric processing of ***iron*** into bioavailable forms that increase the productivity of marine phytoplankton.
- ***Health***

Soil composition

Digital Soil Map of the World



Hybrid STATSGO/FAO Soil Texture



Mean Mineralogical Table (MMT) by Claquin et al., JGR (1999) complemented by Nickovic et al., ACP (2012)

Soil Types	Clay Fraction					Silt Fraction					N	A
	Ill	Kao	Sme	Cal	Qua	Qua	Fel	Cal	Hem	Gyp		
I												
Average	40	20	29	4	7	53	40	6	1	1	6	7
s.d.	13	18	17	4	3	14	12	6	1	1		
Jc												
Average	22	9	46	11	12	31	39	30	0	2	10	2
s.d.	4	3	13	2	3	2	4	3	0	1		
Je												
Average	18	23	55	1	3	86	10	2	1	1	12	1
s.d.	10	11	19	1	2	13	5	2	1	1		
SD												
Average	50	9	26	1	14	92	6	1	1	1	8	12
s.d.	12	5	6	1	4	3	3	1	1	1		
ST												
Average	39	4	26	29	1	5	1	93	1	26	14	3
s.d.	12	3	18	3	1	4	1	27	1	10		

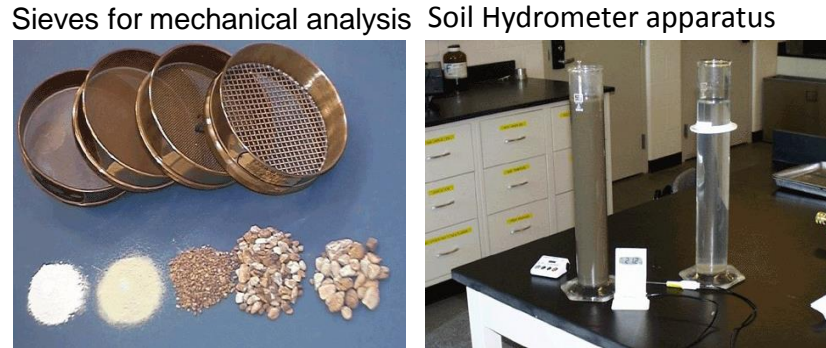
Claquin et al. (1999) proposed that soil mineral content is related to the *soil type* provided by the Digital Soil Map of the World (DSMW)

A recent study has refined the proposed relation between soil type and mineral composition (Journet et al., 2014)

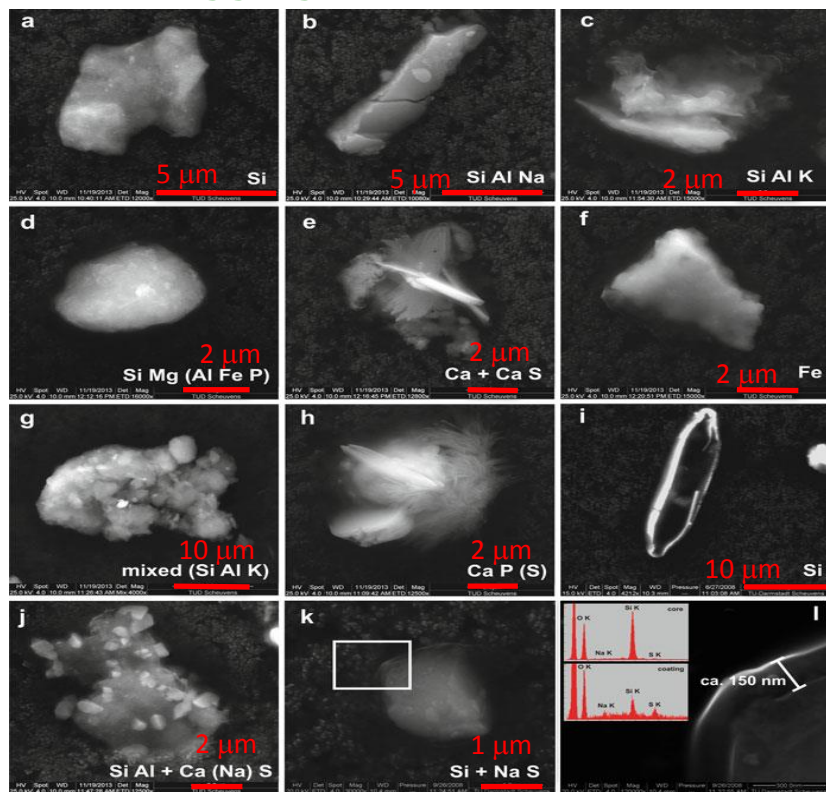
Estimating the soil mineral composition also requires estimates of the fraction of clay and silt-sized particles present at each location, available from global databases of *soil texture*

Challenges for predicting mineral dust composition

Wet sieving in soil analysis



Mineral aggregates/iron oxide impurities



Soil composition extrapolated from a *limited amount of measurements* (particularly scarce in the arid and semi-arid areas that contain dust sources).

Measurements based on *wet sedimentation* (“wet sieving”) techniques that disturb the soil samples, *breaking the aggregates* that are found in the undispersed soil that is subject to wind erosion.

Aggregates partly *fragment* at emission by saltation and sandblasting.

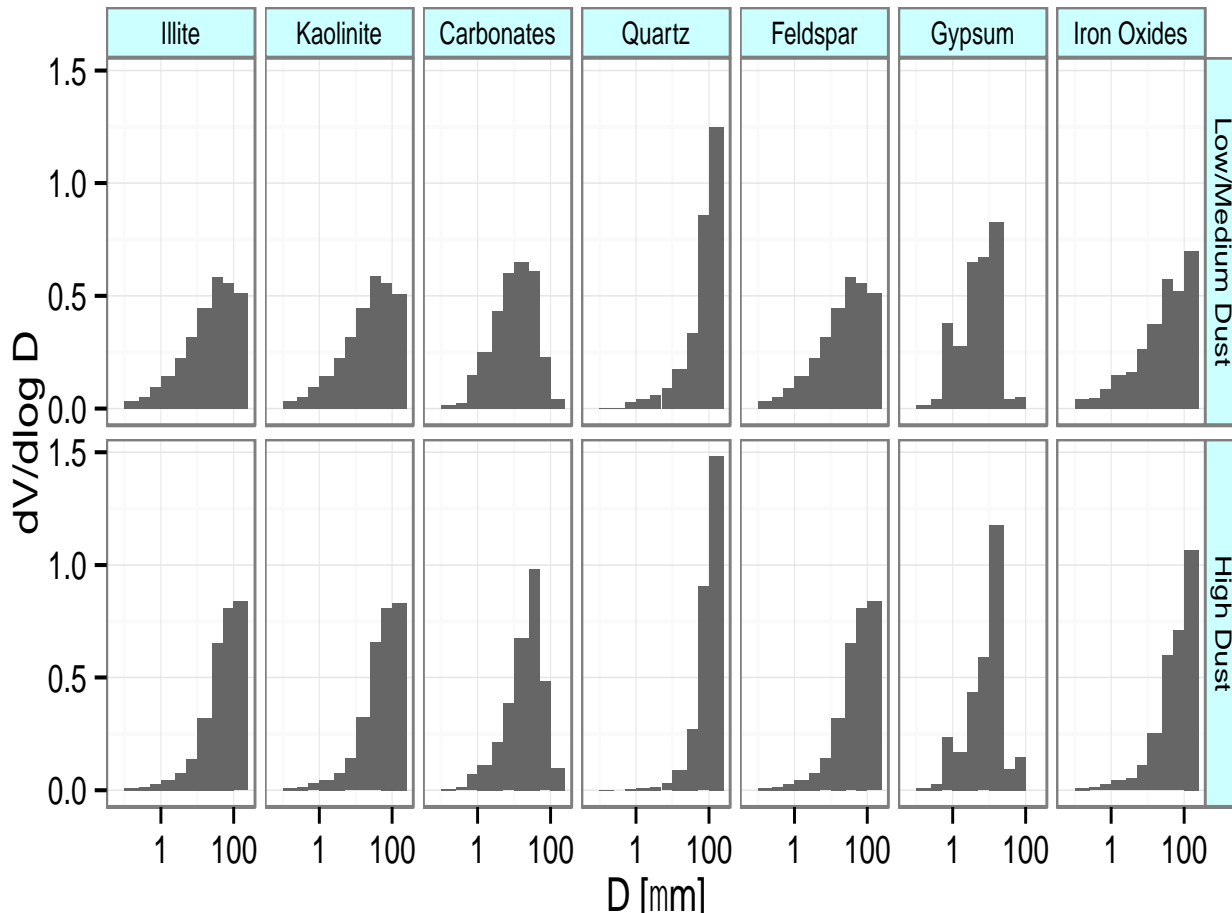
Dust aerosols are composed by *internal and external mixtures* of different minerals

Iron oxides occur as both *small accretions* and pure crystalline forms.

Secondary electron images of typical dust during the SAMUM I campaign in Morocco (Scheuvens and Kandler, 2014)

Observed size distribution

Size distribution of minerals during SAMUM (Kandler et al., 2009)



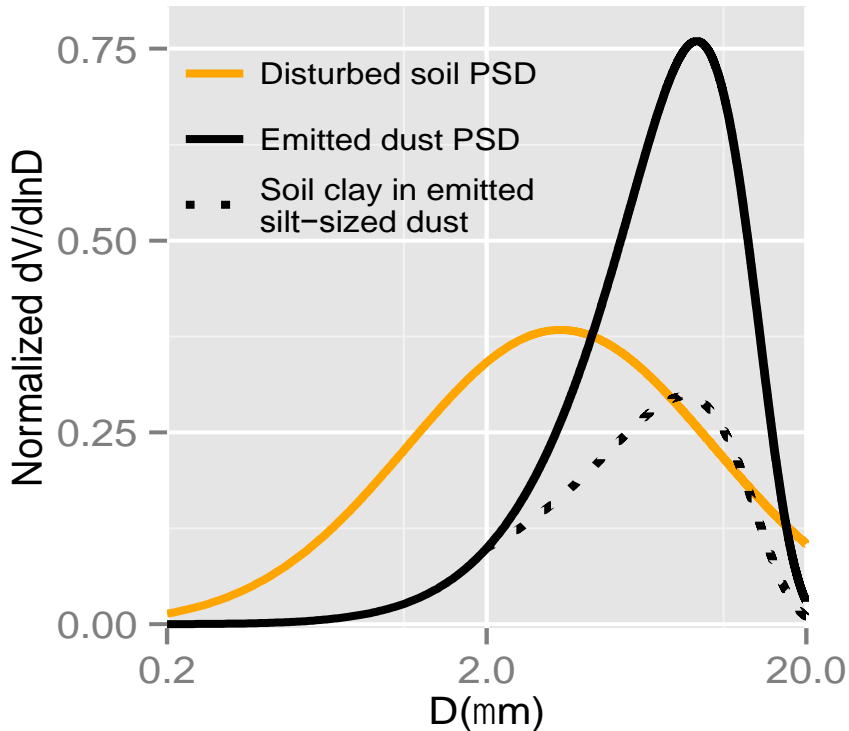
Deduced from single particle analysis as a function of the geometric mean diameter of the corresponding particle size interval

Phyllosilicates abundant at *silt* particle sizes makes clear that many soil aggregates are not broken into clay-sized aerosols during mobilization

Quartz occurs at *larger particle sizes* than other minerals

Different minerals may have *different size distributions in the soil* and may *not be equally susceptible* to *modification* of their size distribution during wet sieving and during the emission process

Constraints Upon the Emitted Size Distribution



Kok (PNAS, 2011)

$$\frac{dV}{d\ln D} = \frac{D}{C_V} u(D) \exp \left[- \left(\frac{D}{\lambda} \right)^3 \right]$$

aggregation brittle fragmentation

Measurements and theory suggest that for sizes $< 15\text{-}20 \mu\text{m}$ the size distribution is approximately invariant, independent of wind speed and soil properties

The net effect of reconstruction of the undispersed soil combined with fragmentation during emission is to *increase the silt-sized fraction at the expense of clay* (the contribution to silt emission from clay-sized soil particles is about half)

We use this invariance to constrain the silt to clay ratio of the emitted dust up to $20 \mu\text{m}$

Because the upper bound of $15\text{-}20 \mu\text{m}$ is mismatched with respect to the MMT (up to $50 \mu\text{m}$), we extrapolate the emitted size distribution using concentration measurements from SAMUM

We constrain the size distribution of each mineral *within* the silt fraction using concentration measurements from SAMUM

Methodology: Soil v. Emitted Mineral Fractions

Wet-sieved soil (Claquin et al., 1999)

$$s^c(b) + s^s(b) = 1 \quad s^c: \text{soil clay fraction}$$

$$s_n^c(a, b) = s^c(b) f_n^c(a) \quad s^s: \text{soil silt fraction}$$

$$f_n^c: \text{fraction of mineral } n \text{ in clay}$$

$$s_n^s(a, b) = s^s(b) f_n^s(a) \quad f_n^s: \text{fraction of mineral } n \text{ in silt}$$

Mineral	Disturbed soil		Undisturbed soil & dust	
	Clay	Silt	Clay	Silt
Illite	●		●	○
Kaolinite	●		●	○
Smectite	●		●	○
Quartz	●	●	●	●
Carbonates	●	●	●	●
Gypsum	●	▷		●
Feldspar	●	▷		●
Iron Oxides	★	●	★	●

Emitted size distribution

Constraint on the emitted silt to clay ratio

$$d^c + d^s = 1$$

d^c : fraction of clay-sized dust

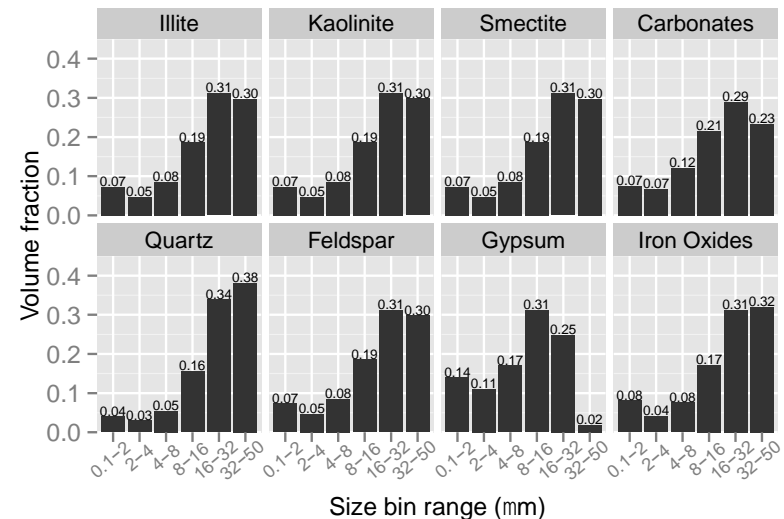
d^s : fraction of silt-sized dust

$$d^s = 1 - d^c = 0.987$$

Aggregation and fragmentation

$$d_n^c(a) = d^c f_n^c(a)$$

$$d_n^s = \eta(\gamma_n s_n^c + s_n^s) \quad \gamma_n: \text{empirical aggregation-fragmentation constant}$$



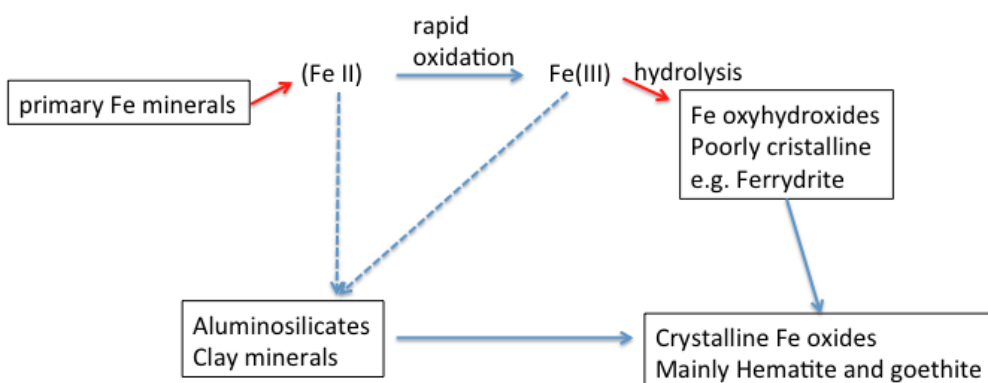
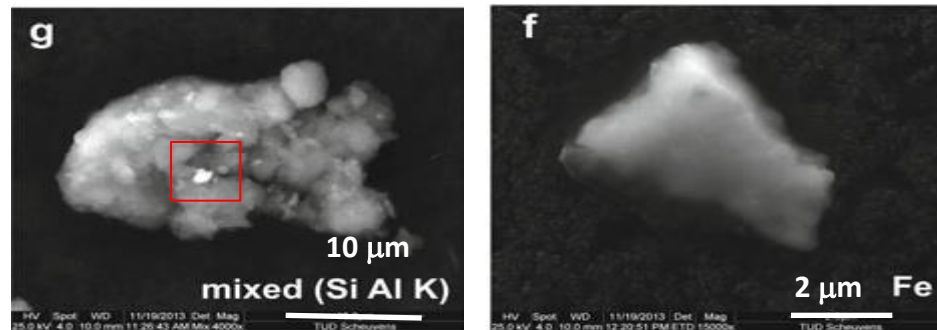
Kandler et al. (2009)

Constrains:

- The sub-silt distribution of each mineral
- Extension of feldspar and gypsum to clay sizes

Methodology: Iron Oxide Accretions

Transport of iron oxides as small impurities



Secondary Fe minerals during chemical weathering

$$d_{Fe,k}^{pure} = \epsilon d_{Fe,k}$$

$$\epsilon = \epsilon_0 d_{Fe,k}$$

$$d_{Fe,k}^{mix} = (1 - \epsilon) d_{Fe,k} = (1 - \epsilon_0 d_{Fe,k}) d_{Fe,k}$$

Iron oxides like hematite are relatively dense and susceptible to gravitational removal. Iron oxides travel farther as *small accretions on the surface of other minerals*.

How to allocate iron oxides between crystalline and accreted form? We assume that the fraction of pure crystalline iron oxide increases where the total iron oxide fraction is large, a heuristic attempt to account for the weathering that creates iron oxides in the soil.

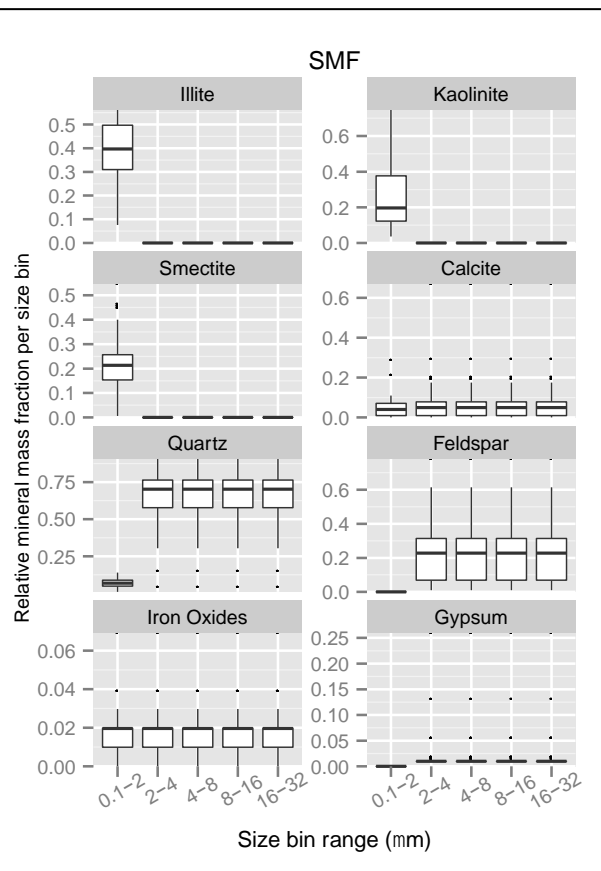
(As soil develops, more of the primary and secondary Fe-bearing minerals decompose and the iron of their lattice structure is converted to iron oxides in the soil: McFadden and Hendricks, 1985; Shi et al., 2012. Micrometer-sized crystalline iron oxide aggregates are typically observed in highly weathered soils that are rich in iron oxides: Chesworth, 2008).

We assume that hematite contributes 5% to the combined particle mass. The remainder of hematite is transported in pure crystalline form.

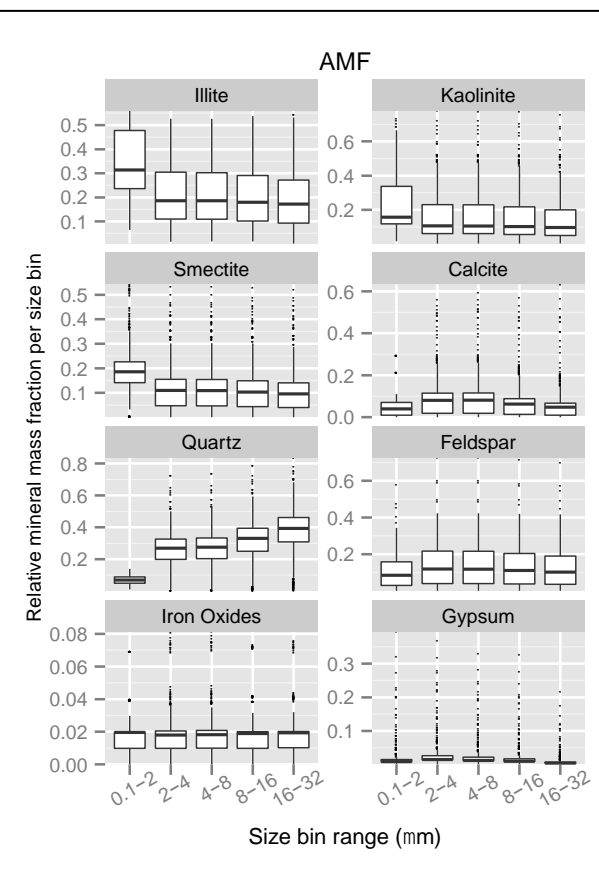
Experiments with GISS ModelE

The soil mass fraction (**SMF**)

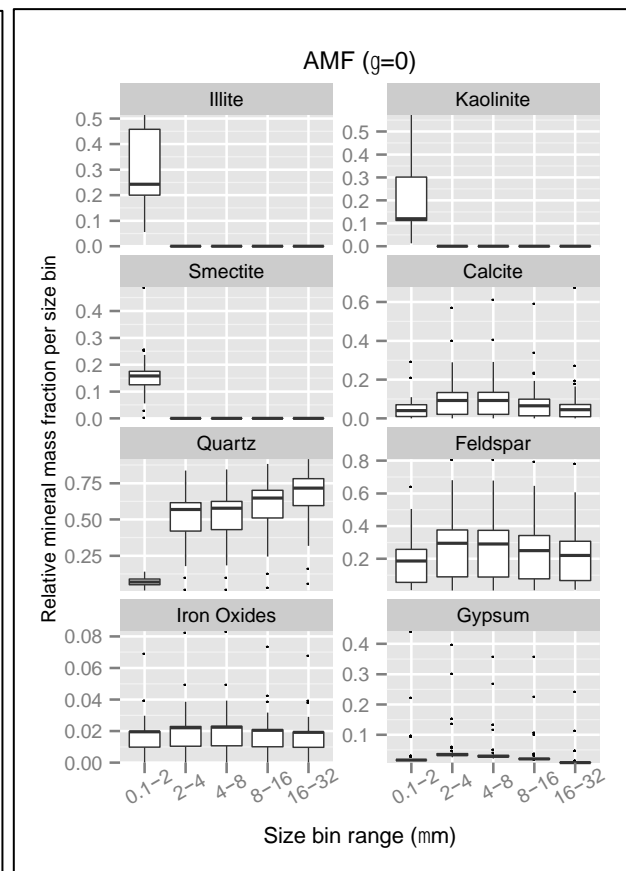
method assumes that the emitted dust mineral content is identical to that of the parent wet-sieved soil



Our new method is the aerosol mass fraction (**AMF**) method
with $\gamma=2$

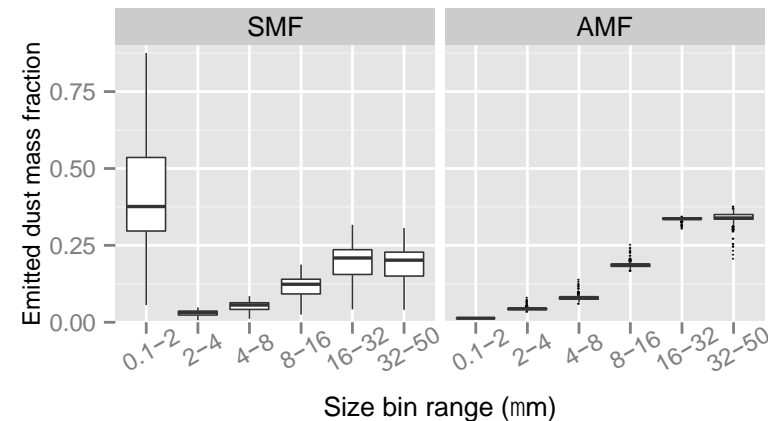
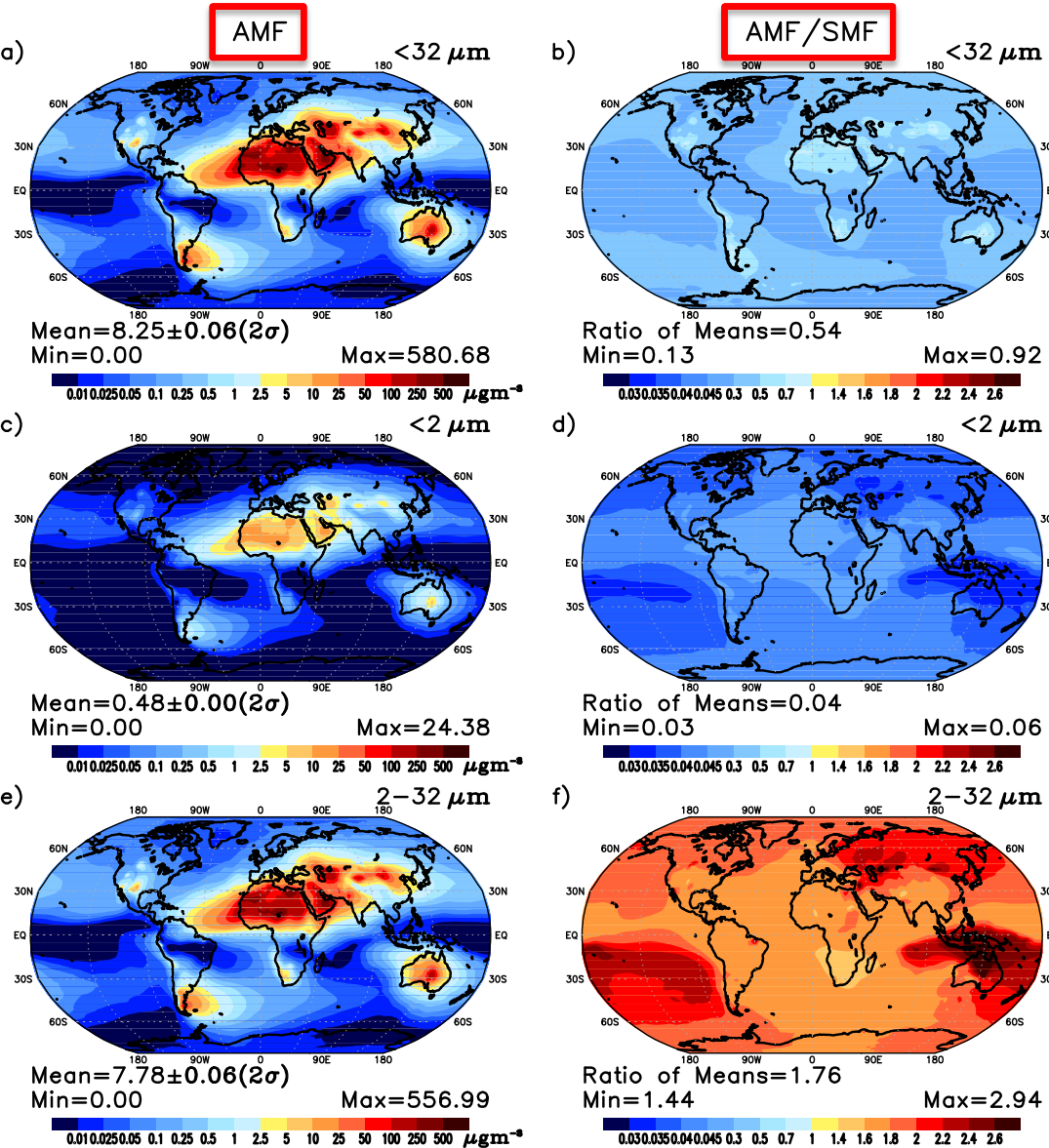


Sensitivity experiments with $\gamma=0$
AMF ($\gamma=0$)



AMF: Aluminosilicates at silt sizes at the expense of clay sizes.
Reduced quartz fraction at silt sizes due to reintroduction of aluminosilicates.

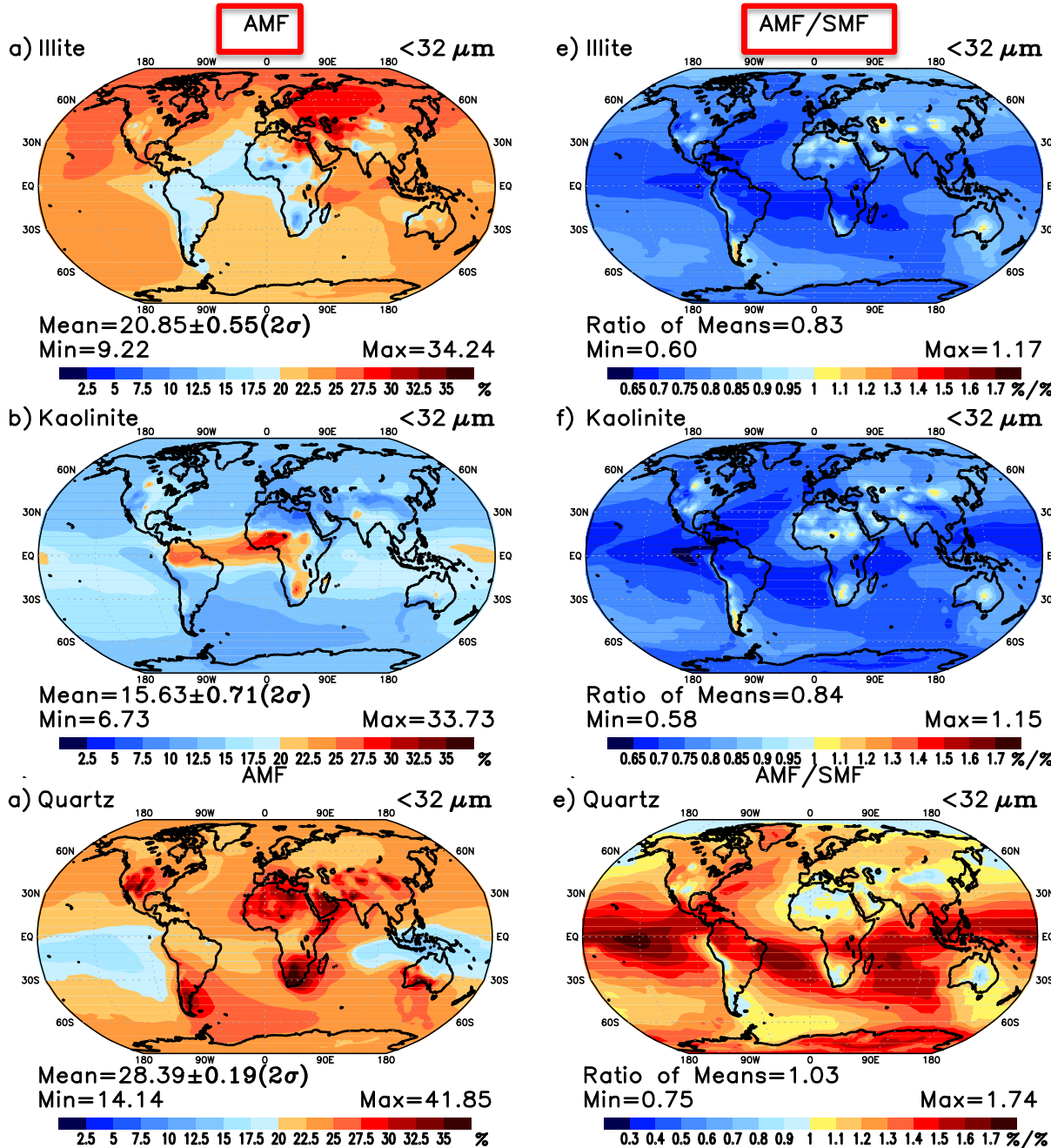
Emitted size distribution and implications for long range transport



SMF: disproportionate fraction of clay-sized emitted aerosols compared to the AMF method.

Important effects upon the simulated dust concentration: in the **AMF**, silt-sized particles are deposited closer to the source through gravitational removal

Global mineral fractions: Surface Concentration



Aluminosilicates

AMF shows 15% reduction on average compared to the SMF

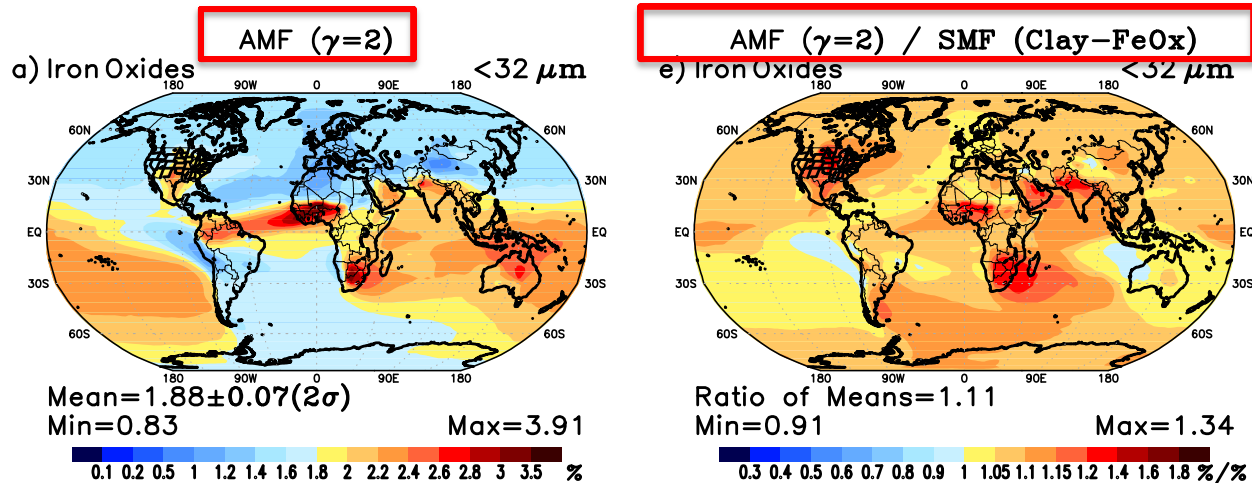
Due to redistribution of mass from the clay to the silt size range along with the faster sedimentation of large silt particles.

Quartz

Although the AMF method decreases the quartz fraction in the silt size range, the emitted silt mass is larger.

Enhancements largest in remote regions. Increases are generally smaller close to source regions.

Iron oxides

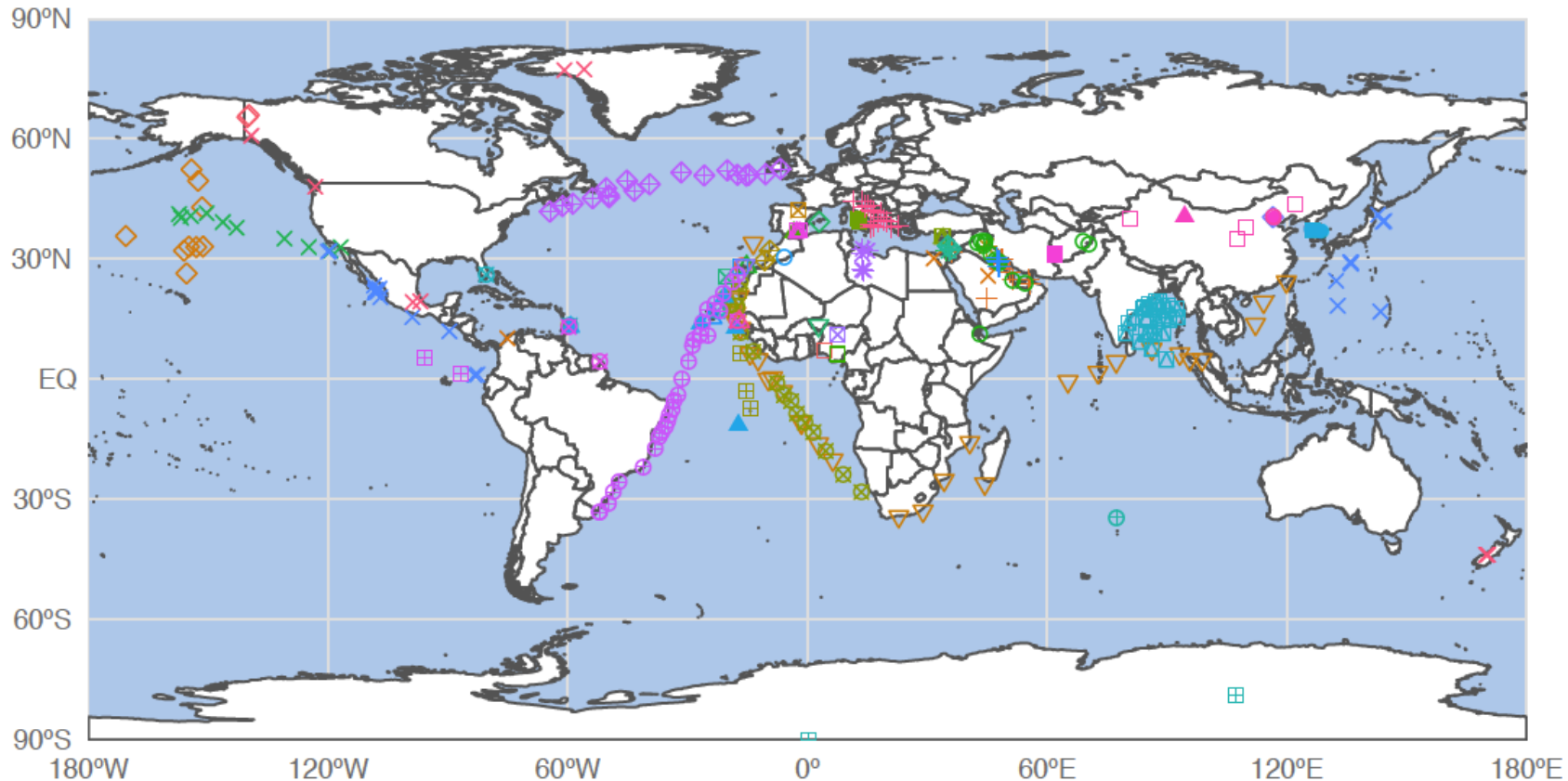


Two competing effects:

1. The SMF method emits more clay. This size has a longer lifetime and trajectory. However, the iron oxides are only in dense crystalline form.
2. The AMF method emits more silt-sized iron oxides, but some is present as accretions on the other minerals that are relatively buoyant.

The AMF accretions allow greater dispersion of iron from the source.

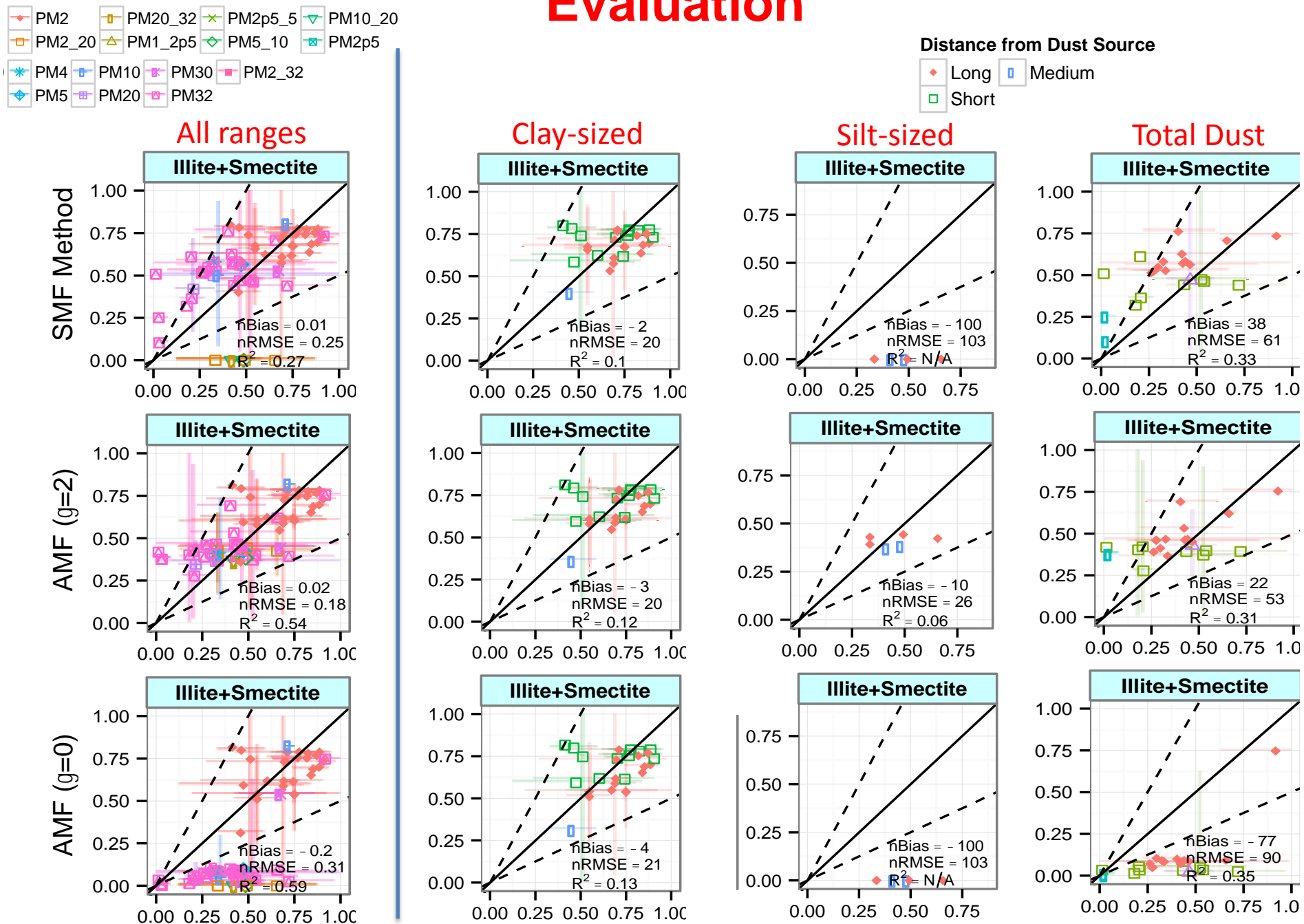
Evaluation



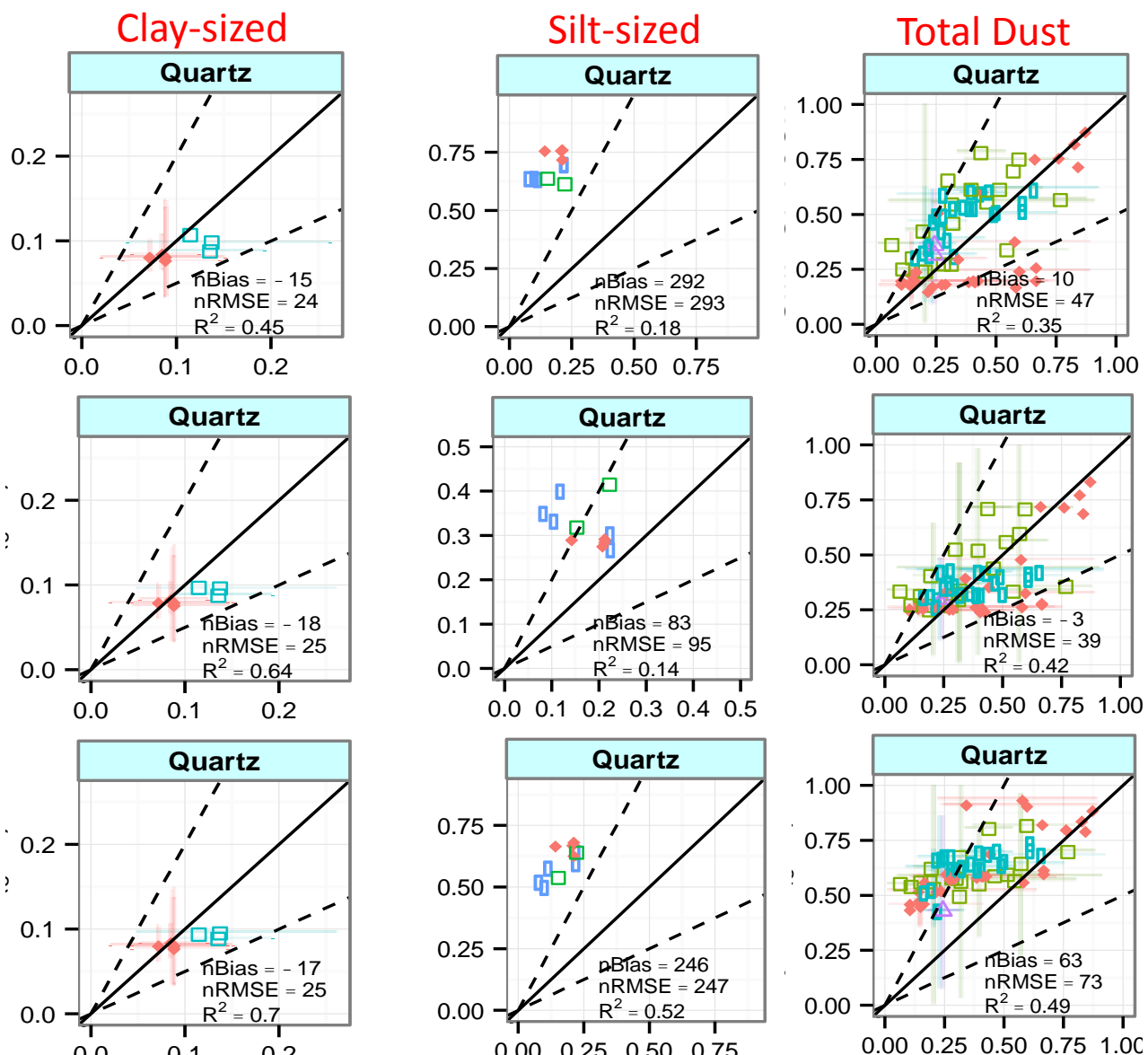
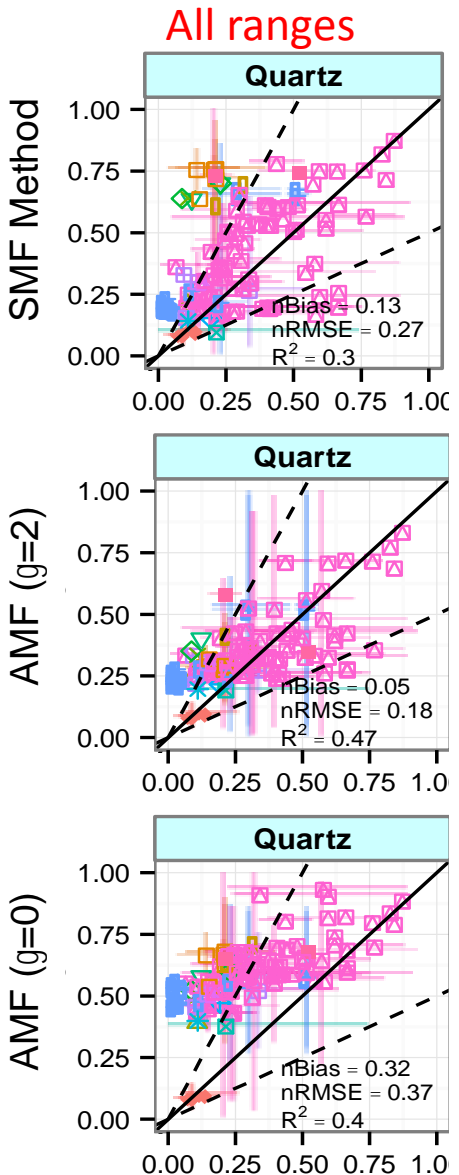
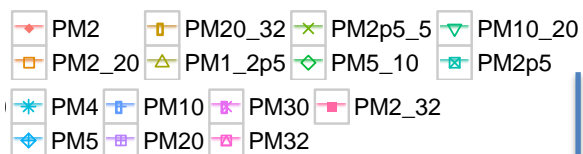
Reference

- | | | | |
|--|---|---|--|
| □ Adedokum et al. (1989):7.29°N,4.34°E | ● Delany et al. (1967):13.17°N,59.42°W | □ Goldberg and Griffin (1970) | ■ Prospero and Bonatti (1969) |
| ○ Alastuey et al. (2005) | ▲ Diaz-Hernández et al. (2011):37.17°N,3.52°W | ■ Jeong (2008):37.5°N,126.92°E | ■ Prospero et al. (1981) |
| △ Al-Awadhi and Al-Shuaibi (2013) | □ Enete et al. (2012) | ● Jeong et al. (2014) | □ Queralt-Mitjans et al. (1993) |
| + Al-Dousari and Al-Awadhi (2012) | ● Engelbrecht et al. (2009) | ▲ Johnson (1976) | ■ Rashki et al. (2013) |
| × Al-Dousari et al. (2013) | △ Engelbrecht et al. (2014):28.07°N,15.45°W | □ Kandler et al. (2007):28.32°N,16.5°W | ● Shao et al. (2008):39.99°N,116.34°E |
| ◇ Arnold et al. (1998) | + Falkovich et al. (2001):32.08°N,34.8°E | ○ Kandler et al. (2009):30.24°N,5.6°W | ▲ Shen et al., (2006):40.5°N,94.82°E |
| ▽ Aston et al. (1973) | × Ferguson et al. (1970) | △ Kandler et al. (2011):14.94°N,23.48°W | □ Shen et al. (2009) |
| ■ Avila et al. (1997):41.77°N,2.35°W | ◇ Fiol et al. (2005):39.63°N,2.65°E | ⊕ Khalaf et al. (1985) | ○ Shi et al. (2005):40°N,116.77°E |
| * Awadh (2012):33.33°N,44.43°E | ▽ Formenti et al. (2008):13.5°N,2.6°E | × Leinen et al. (1994) | △ Skonieczny et al. (2013):14.41°N,16.96°W |
| ◆ Chester and Johnson (1971a) | ■ Game (1964):25.07°N,20.73°W | ◇ Lu et al. (2006):40°N,116.77°E | + |
| ◆ Chester and Johnson (1971b) | ● Ganor (1991):31.78°N,35.22°E | ▽ Menendez et al. (2007):27.97°N,15.6°W | □ Tomadin et al. (1984) |
| ■ Chester et al. (1971) | ◇ Gaudichet et al. (2000) | ■ Møberg et al. (1991):11.07°N,7.7°E | × Windom (1969) |
| ■ Chester et al. (1972) | ● Gaudichet et al. (1989):34.78°S,77.52°E | ● O'Hara et al. (2006) | ◇ Zdanowicz et al. (2006) |
| ■ Chester et al. (1977) | ● Gaudichet et al. (1992) | ● Parkin et al. (1970) | |
| ■ Chester et al. (1984) | ● Glaccum and Prospero (1980) | ● Parkin et al. (1972) | |

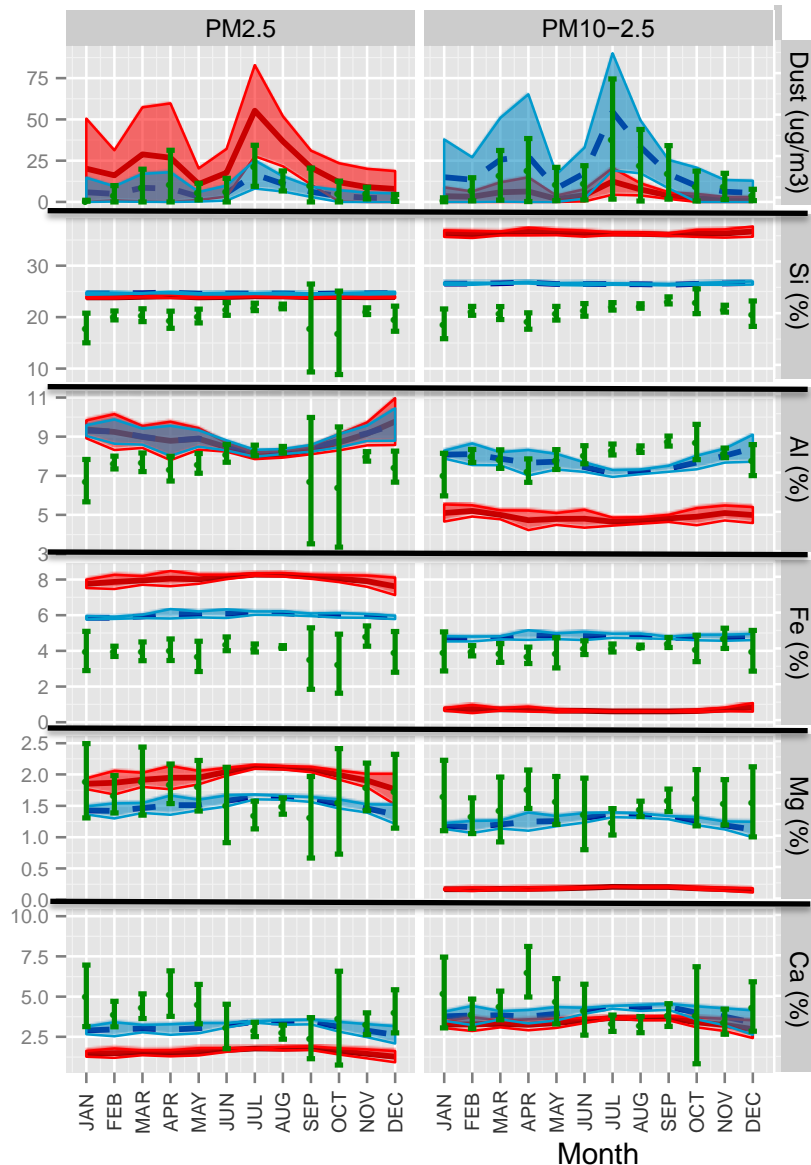
Evaluation



Evaluation



Evaluation



Elemental Composition (Measured Data at Izana 2002-2010, Provided by Sergio Rodriguez, Izaña Atmospheric Research Centre)

Conclusions and future

- Our semi-empirical method accounts for soil aggregation and aggregate fragmentation at emission.
- Despite the limited observations and the uncertainties in evaluation we show robust improvements in the description of the dust mineral distribution.
- Our treatment of hematite is subject to relatively few observational constraints and amenable to more precise future treatments.
- Method to be tested with a new soil composition database (Journet et al., 2014)
- We are working on a theoretical method of the emitted fractions.
- We make available our compilation of observations along with their uncertainties for comparison with other climate models.
- 2 papers about to be submitted (Perlitz et al., 2014a,b) and 1 paper in preparation (Pérez García-Pando et al., in prep)